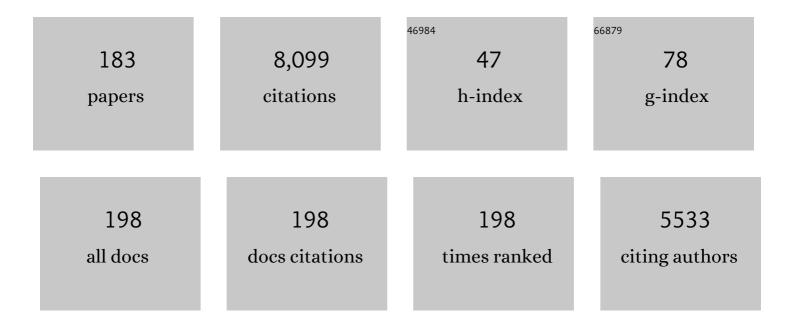
Zhou Shi

List of Publications by Year in descending order

Source: https://exaly.com/author-pdf/9055186/publications.pdf Version: 2024-02-01



#	Article	IF	CITATIONS
1	Comprehensive source identification and apportionment analysis of five heavy metals in soils in Wenzhou City, China. Environmental Geochemistry and Health, 2022, 44, 579-602.	1.8	14
2	Significant loss of soil inorganic carbon at the continental scale. National Science Review, 2022, 9, nwab120.	4.6	34
3	Mapping high resolution National Soil Information Grids of China. Science Bulletin, 2022, 67, 328-340.	4.3	161
4	Digital mapping of GlobalSoilMap soil properties at a broad scale: A review. Geoderma, 2022, 409, 115567.	2.3	167
5	Identification and risk prediction of potentially contaminated sites in the Yangtze River Delta. Science of the Total Environment, 2022, 815, 151982.	3.9	20
6	A framework for determining the total salt content of soil profiles using time-series Sentinel-2 images and a random forest-temporal convolution network. Geoderma, 2022, 409, 115656.	2.3	20
7	Soil organic carbon storage, distribution, and influencing factors at different depths in the dryland farming regions of Northeast and North China. Catena, 2022, 210, 105934.	2.2	18
8	Fusion of visible-to-near-infrared and mid-infrared spectroscopy to estimate soil organic carbon. Soil and Tillage Research, 2022, 217, 105284.	2.6	21
9	Drivers of water erosion-induced lateral soil carbon loss on the Tibetan Plateau. Catena, 2022, 211, 105970.	2.2	7
10	Role of Environment Variables in Spatial Distribution of Soil C, N, P Ecological Stoichiometry in the Typical Black Soil Region of Northeast China. Sustainability, 2022, 14, 2636.	1.6	5
11	Strategies for efficient estimation of soil organic content at the local scale based on a national spectral database. Land Degradation and Development, 2022, 33, 1649-1661.	1.8	6
12	Pollution Assessment and Source Apportionment of Soil Heavy Metals in a Coastal Industrial City, Zhejiang, Southeastern China. International Journal of Environmental Research and Public Health, 2022, 19, 3335.	1.2	19
13	Predicting annual PM2.5 in mainland China from 2014 to 2020 using multi temporal satellite product: An improved deep learning approach with spatial generalization ability. ISPRS Journal of Photogrammetry and Remote Sensing, 2022, 187, 141-158.	4.9	19
14	Estimating soil bacterial abundance and diversity in the Southeast Qinghai-Tibet Plateau. Geoderma, 2022, 416, 115807.	2.3	4
15	Decoupling environmental impact from economic growth to achieve Sustainable Development Goals in China. Journal of Environmental Management, 2022, 312, 114978.	3.8	27
16	Extraction of Agricultural Fields via DASFNet with Dual Attention Mechanism and Multi-scale Feature Fusion in South Xinjiang, China. Remote Sensing, 2022, 14, 2253.	1.8	15
17	Deep transfer learning of global spectra for local soil carbon monitoring. ISPRS Journal of Photogrammetry and Remote Sensing, 2022, 188, 190-200.	4.9	26
18	Integrating social media and field investigations to monitor contaminated sites. Journal of Cleaner Production, 2022, 358, 132072.	4.6	3

#	Article	IF	CITATIONS
19	Source Identification and Apportionment of Potential Toxic Elements in Soils in an Eastern Industrial City, China. International Journal of Environmental Research and Public Health, 2022, 19, 6132.	1.2	3
20	Improving remote sensing of salinity on topsoil with crop residues using novel indices of optical and microwave bands. Geoderma, 2022, 422, 115935.	2.3	6
21	Digital Mapping of Soil Organic Carbon with Machine Learning in Dryland of Northeast and North Plain China. Remote Sensing, 2022, 14, 2504.	1.8	9
22	Climate-induced shifts in composition and protection regulate temperature sensitivity of carbon decomposition through soil profile. Soil Biology and Biochemistry, 2022, 172, 108743.	4.2	14
23	Assessment of three gridded satellite-based precipitation products and their performance variabilities during typhoons over Zhejiang, southeastern China. Journal of Hydrology, 2022, 610, 127985.	2.3	9
24	Mapping the Levels of Soil Salination and Alkalization by Integrating Machining Learning Methods and Soil-Forming Factors. Remote Sensing, 2022, 14, 3020.	1.8	3
25	Relative Strengths Recognition of Nine Mainstream Satellite-Based Soil Moisture Products at the Global Scale. Remote Sensing, 2022, 14, 2739.	1.8	4
26	Younger carbon dominates global soil carbon efflux. Global Change Biology, 2022, 28, 5587-5599.	4.2	12
27	Preliminary risk assessment of regional industrial enterprise sites based on big data. Science of the Total Environment, 2022, 838, 156609.	3.9	9
28	Stoichiometry of soil carbon, nitrogen, and phosphorus in farmland soils in southern China: Spatial pattern and related dominates. Catena, 2022, 217, 106468.	2.2	24
29	Diffuse reflectance spectroscopy for estimating soil properties: A technology for the 21st century. European Journal of Soil Science, 2022, 73, .	1.8	30
30	Effectiveness of different approaches for in situ measurements of organic carbon using visible and near infrared spectrometry in the Poyang Lake basin area. Land Degradation and Development, 2021, 32, 1301-1311.	1.8	8
31	VIRS based detection in combination with machine learning for mapping soil pollution. Environmental Pollution, 2021, 268, 115845.	3.7	38
32	Assessment of potentially toxic element pollution in soils and related health risks in 271 cities across China. Environmental Pollution, 2021, 270, 116196.	3.7	46
33	Revealing the scale- and location-specific controlling factors of soil organic carbon in Tibet. Geoderma, 2021, 382, 114713.	2.3	39
34	Novel framework for modelling the cadmium balance and accumulation in farmland soil in Zhejiang Province, East China: Sensitivity analysis, parameter optimisation, and forecast for 2050. Journal of Cleaner Production, 2021, 279, 123674.	4.6	23
35	Current Status and Temporal Trend of Potentially Toxic Elements Pollution in Agricultural Soil in the Yangtze River Delta Region: A Meta-Analysis. International Journal of Environmental Research and Public Health, 2021, 18, 1033.	1.2	10
36	Sea Surface Salinity Estimation and Spatial-Temporal Heterogeneity Analysis in the Gulf of Mexico. Remote Sensing, 2021, 13, 881.	1.8	6

#	Article	IF	CITATIONS
37	Estimation and Mapping of Soil Properties Based on Multi-Source Data Fusion. Remote Sensing, 2021, 13, 978.	1.8	8
38	Predicting Bioaccumulation of Potentially Toxic Element in Soil–Rice Systems Using Multi-Source Data and Machine Learning Methods: A Case Study of an Industrial City in Southeast China. Land, 2021, 10, 558.	1.2	14
39	High-resolution prediction of the spatial distribution of PM2.5 concentrations in China using a long short-term memory model. Journal of Cleaner Production, 2021, 297, 126493.	4.6	18
40	Climate change-induced greening on the Tibetan Plateau modulated by mountainous characteristics. Environmental Research Letters, 2021, 16, 064064.	2.2	16
41	An integrated assessment methodology for management of potentially contaminated sites based on public data. Science of the Total Environment, 2021, 783, 146913.	3.9	21
42	Evaluating validation strategies on the performance of soil property prediction from regional to continental spectral data. Geoderma, 2021, 400, 115159.	2.3	32
43	Diagnosis of cadmium contamination in urban and suburban soils using visible-to-near-infrared spectroscopy. Environmental Pollution, 2021, 291, 118128.	3.7	26
44	A Super Typhoon Disturbs Organic Contamination in Agricultural Soils. Environmental Science and Technology Letters, 2021, 8, 237-243.	3.9	6
45	Dynamics of Vegetation Greenness and Its Response to Climate Change in Xinjiang over the Past Two Decades. Remote Sensing, 2021, 13, 4063.	1.8	19
46	Life cycle assessment and fertilization scheme optimization of paddy field crops in South China. Journal of Cleaner Production, 2021, 325, 129339.	4.6	9
47	Monitoring soil organic carbon in alpine soils using in situ visâ€NIR spectroscopy and a multilayer perceptron. Land Degradation and Development, 2020, 31, 1026-1038.	1.8	37
48	Composite assessment of human health risk from potentially toxic elements through multiple exposure routes: A case study in farmland in an important industrial city in East China. Journal of Geochemical Exploration, 2020, 210, 106443.	1.5	37
49	Updated information on soil salinity in a typical oasis agroecosystem and desert-oasis ecotone: Case study conducted along the Tarim River, China. Science of the Total Environment, 2020, 716, 135387.	3.9	21
50	Improved Mapping of Potentially Toxic Elements in Soil via Integration of Multiple Data Sources and Various Geostatistical Methods. Remote Sensing, 2020, 12, 3775.	1.8	16
51	Estimating spatial and temporal variation in ocean surface pCO2 in the Gulf of Mexico using remote sensing and machine learning techniques. Science of the Total Environment, 2020, 745, 140965.	3.9	17
52	Interactive effects of elevation and land use on soil bacterial communities in the Tibetan Plateau. Pedosphere, 2020, 30, 817-831.	2.1	21
53	Road Extraction from Very-High-Resolution Remote Sensing Images via a Nested SE-Deeplab Model. Remote Sensing, 2020, 12, 2985.	1.8	49
54	Integrating Remote Sensing and Landscape Characteristics to Estimate Soil Salinity Using Machine Learning Methods: A Case Study from Southern Xinjiang, China. Remote Sensing, 2020, 12, 4118.	1.8	44

#	Article	IF	CITATIONS
55	Data fusion for the measurement of potentially toxic elements in soil using portable spectrometers. Environmental Pollution, 2020, 263, 114649.	3.7	36
56	Rapid Determination of Soil Class Based on Visible-Near Infrared, Mid-Infrared Spectroscopy and Data Fusion. Remote Sensing, 2020, 12, 1512.	1.8	25
57	Distinct controls over the temporal dynamics of soil carbon fractions after land use change. Global Change Biology, 2020, 26, 4614-4625.	4.2	48
58	Current status, spatial features, health risks, and potential driving factors of soil heavy metal pollution in China at province level. Environmental Pollution, 2020, 266, 114961.	3.7	257
59	Modelling bioaccumulation of heavy metals in soil-crop ecosystems and identifying its controlling factors using machine learning. Environmental Pollution, 2020, 262, 114308.	3.7	126
60	Spatial-temporal distribution of carbon emissions by daily travel and its response to urban form: A case study of Hangzhou, China. Journal of Cleaner Production, 2020, 257, 120797.	4.6	64
61	Spatio-temporal variation and source changes of potentially toxic elements in soil on a typical plain of the Yangtze River Delta, China (2002–2012). Journal of Environmental Management, 2020, 271, 110943.	3.8	41
62	Identification of the potential risk areas for soil heavy metal pollution based on the source-sink theory. Journal of Hazardous Materials, 2020, 393, 122424.	6.5	133
63	Fine-Resolution Mapping of Soil Total Nitrogen across China Based on Weighted Model Averaging. Remote Sensing, 2020, 12, 85.	1.8	31
64	Three-dimensional digital soil mapping of multiple soil properties at a field-scale using regression kriging. Geoderma, 2020, 366, 114253.	2.3	44
65	A comprehensive framework for assessing the impact of potential agricultural pollution on grain security and human health in economically developed areas. Environmental Pollution, 2020, 263, 114653.	3.7	35
66	Multi-algorithm comparison for predicting soil salinity. Geoderma, 2020, 365, 114211.	2.3	79
67	AIMERG: a new Asian precipitation dataset (0.1°/half-hourly, 2000–2015) by calibrating the GPM-era IMERG at a daily scale using APHRODITE. Earth System Science Data, 2020, 12, 1525-1544.	3.7	75
68	Rapid determination of soil classes in soil profiles using vis–NIR spectroscopy and multiple objectives mixed support vector classification. European Journal of Soil Science, 2019, 70, 42-53.	1.8	21
69	Multiâ€sensor fusion for the determination of several soil properties in the Yangtze River Delta, China. European Journal of Soil Science, 2019, 70, 162-173.	1.8	79
70	Estimating soil salinity from remote sensing and terrain data in southern Xinjiang Province, China. Geoderma, 2019, 337, 1309-1319.	2.3	200
71	National digital soil map of organic matter in topsoil and its associated uncertainty in 1980's China. Geoderma, 2019, 335, 47-56.	2.3	80
72	Land use and climate change effects on soil organic carbon in North and Northeast China. Science of the Total Environment, 2019, 647, 1230-1238.	3.9	138

#	Article	IF	CITATIONS
73	Baseline map of soil organic carbon in Tibet and its uncertainty in the 1980s. Geoderma, 2019, 334, 124-133.	2.3	35
74	Using Nighttime Light Data and POI Big Data to Detect the Urban Centers of Hangzhou. Remote Sensing, 2019, 11, 1821.	1.8	40
75	Improvement of Spatial Modeling of Cr, Pb, Cd, As and Ni in Soil Based on Portable X-ray Fluorescence (PXRF) and Geostatistics: A Case Study in East China. International Journal of Environmental Research and Public Health, 2019, 16, 2694.	1.2	30
76	Spatial and Temporal Variations in the Rainy Season Onset over the Qinghai–Tibet Plateau. Water (Switzerland), 2019, 11, 1960.	1.2	8
77	Modelling and mapping soil erosion potential in China. Journal of Integrative Agriculture, 2019, 18, 251-264.	1.7	73
78	Simultaneous measurement of multiple soil properties through proximal sensor data fusion: A case study. Geoderma, 2019, 341, 111-128.	2.3	73
79	Evaluation of Machine Learning Approaches to Predict Soil Organic Matter and pH Using vis-NIR Spectra. Sensors, 2019, 19, 263.	2.1	91
80	Analyzing spatial patterns of urban carbon metabolism and its response to change of urban size: A case of the Yangtze River Delta, China. Ecological Indicators, 2019, 104, 615-625.	2.6	69
81	Characterising dryland salinity in three dimensions. Science of the Total Environment, 2019, 682, 190-199.	3.9	34
82	X-ray fluorescence and visible near infrared sensor fusion for predicting soil chromium content. Geoderma, 2019, 352, 61-69.	2.3	57
83	High-resolution three-dimensional mapping of soil organic carbon in China: Effects of SoilGrids products on national modeling. Science of the Total Environment, 2019, 685, 480-489.	3.9	66
84	Quantitative Estimation of Soil Salinity Using UAV-Borne Hyperspectral and Satellite Multispectral Images. Remote Sensing, 2019, 11, 736.	1.8	87
85	A new approach for obtaining precipitation estimates with a finer spatial resolution on a daily scale based on TMPA V7 data over the Tibetan Plateau. International Journal of Remote Sensing, 2019, 40, 8465-8483.	1.3	17
86	Estimating forest soil organic carbon content using vis-NIR spectroscopy: Implications for large-scale soil carbon spectroscopic assessment. Geoderma, 2019, 348, 37-44.	2.3	70
87	Integrating a Hybrid Back Propagation Neural Network and Particle Swarm Optimization for Estimating Soil Heavy Metal Contents Using Hyperspectral Data. Sustainability, 2019, 11, 419.	1.6	35
88	A methodological framework for identifying potential sources of soil heavy metal pollution based on machine learning: A case study in the Yangtze Delta, China. Environmental Pollution, 2019, 250, 601-609.	3.7	101
89	Quantitative Evaluations and Error Source Analysis of Fengyun-2-Based and GPM-Based Precipitation Products over Mainland China in Summer, 2018. Remote Sensing, 2019, 11, 2992.	1.8	40
90	Identifying heavy metal pollution hot spots in soil-rice systems: A case study in South of Yangtze River Delta, China. Science of the Total Environment, 2019, 658, 614-625.	3.9	90

Zнои Sні

#	Article	IF	CITATIONS
91	A high-resolution map of soil pH in China made by hybrid modelling of sparse soil data and environmental covariates and its implications for pollution. Science of the Total Environment, 2019, 655, 273-283.	3.9	124
92	Soil bacterial abundance and diversity better explained and predicted with spectro-transfer functions. Soil Biology and Biochemistry, 2019, 129, 29-38.	4.2	23
93	Editorial for pedometrics 2017 special issue. European Journal of Soil Science, 2019, 70, 25-26.	1.8	0
94	Updating a national soil classification with spectroscopic predictions and digital soil mapping. Catena, 2018, 164, 125-134.	2.2	47
95	Proximal and remote sensing techniques for mapping of soil contamination with heavy metals. Applied Spectroscopy Reviews, 2018, 53, 783-805.	3.4	51
96	Improving TMPA 3B43 V7 Data Sets Using Land-Surface Characteristics and Ground Observations on the Qinghai–Tibet Plateau. IEEE Geoscience and Remote Sensing Letters, 2018, 15, 178-182.	1.4	20
97	Current and future assessments of soil erosion by water on the Tibetan Plateau based on RUSLE and CMIP5 climate models. Science of the Total Environment, 2018, 635, 673-686.	3.9	184
98	Spatial and temporal precipitation patterns characterized by TRMM TMPA over the Qinghai-Tibetan plateau and surroundings. International Journal of Remote Sensing, 2018, 39, 3891-3907.	1.3	37
99	Identifying scale-specific controls of soil organic matter distribution in mountain areas using anisotropy analysis and discrete wavelet transform. Catena, 2018, 160, 1-9.	2.2	13
100	Assessment of important soil properties related to Chinese Soil Taxonomy based on vis–NIR reflectance spectroscopy. Computers and Electronics in Agriculture, 2018, 144, 1-8.	3.7	58
101	A Methodological Framework to Retrospectively Obtain Downscaled Precipitation Estimates over the Tibetan Plateau. Remote Sensing, 2018, 10, 1974.	1.8	7
102	Application of Spectrally Derived Soil Type as Ancillary Data to Improve the Estimation of Soil Organic Carbon by Using the Chinese Soil Vis-NIR Spectral Library. Remote Sensing, 2018, 10, 1747.	1.8	31
103	A robust method to estimate foliar phosphorus of rubber trees with hyperspectral reflectance. Industrial Crops and Products, 2018, 126, 1-12.	2.5	17
104	Improving Spatial Soil Moisture Representation through the Integration of SMAP and PROBA-V Products. Sustainability, 2018, 10, 3459.	1.6	1
105	Integrating multi-source data to improve water erosion mapping in Tibet, China. Catena, 2018, 169, 31-45.	2.2	25
106	Identifying localized and scale-specific multivariate controls of soil organic matter variations using multiple wavelet coherence. Science of the Total Environment, 2018, 643, 548-558.	3.9	30
107	Geo-detection of factors controlling spatial patterns of heavy metals in urban topsoil using multi-source data. Science of the Total Environment, 2018, 643, 451-459.	3.9	72
108	The assessment of soil erosion risk, sediment yield and their controlling factors on a large scale: Example of Morocco. Journal of African Earth Sciences, 2018, 147, 281-299.	0.9	35

Zнои Sні

#	Article	IF	CITATIONS
109	Estimation Methods for Soil Mercury Content Using Hyperspectral Remote Sensing. Sustainability, 2018, 10, 2474.	1.6	46
110	Source Identification and Apportionment of Trace Elements in Soils in the Yangtze River Delta, China. International Journal of Environmental Research and Public Health, 2018, 15, 1240.	1.2	30
111	Heavy Metal Pollution Delineation Based on Uncertainty in a Coastal Industrial City in the Yangtze River Delta, China. International Journal of Environmental Research and Public Health, 2018, 15, 710.	1.2	42
112	Quantifying the spatial patterns of urban carbon metabolism: A case study of Hangzhou, China. Ecological Indicators, 2018, 95, 474-484.	2.6	50
113	Downscaling annual precipitation with <scp>TMPA</scp> and land surface characteristics in China. International Journal of Climatology, 2017, 37, 5107-5119.	1.5	41
114	A spatial data mining algorithm for downscaling TMPA 3B43 V7 data over the Qinghai–Tibet Plateau with the effects of systematic anomalies removed. Remote Sensing of Environment, 2017, 200, 378-395.	4.6	124
115	Organic carbon prediction in soil cores using VNIR and MIR techniques in an alpine landscape. Scientific Reports, 2017, 7, 2144.	1.6	37
116	Assessment of the potential health risks of heavy metals in soils in a coastal industrial region of the Yangtze River Delta. Environmental Science and Pollution Research, 2017, 24, 19816-19826.	2.7	78
117	Improving Rainfall Erosivity Estimates Using Merged TRMM and Gauge Data. Remote Sensing, 2017, 9, 1134.	1.8	27
118	Decomposed Driving Factors of Carbon Emissions and Scenario Analyses of Low-Carbon Transformation in 2020 and 2030 for Zhejiang Province. Energies, 2017, 10, 1747.	1.6	31
119	Application of portable XRF and VNIR sensors for rapid assessment of soil heavy metal pollution. PLoS ONE, 2017, 12, e0172438.	1.1	94
120	An Integrated Approach to Explore the Relationship Among Economic, Construction Land Use, and Ecology Subsystems in Zhejiang Province, China. Sustainability, 2016, 8, 498.	1.6	9
121	Precipitation change between 1960 and 2006 in the Qiantang River basin, eastern China. Climate Research, 2016, 67, 257-269.	0.4	4
122	Predicting total dissolved salts and soluble ion concentrations in agricultural soils using portable visible near-infrared and mid-infrared spectrometers. Biosystems Engineering, 2016, 152, 94-103.	1.9	43
123	Supplemental sampling for digital soil mapping based on prediction uncertainty from both the feature domain and the spatial domain. Geoderma, 2016, 284, 73-84.	2.3	16
124	Revealing the scale-specific controls of soil organic matter at large scale in Northeast and North China Plain. Geoderma, 2016, 271, 71-79.	2.3	57
125	Assessment of soil properties in situ using a prototype portable MIR spectrometer in two agricultural fields. Biosystems Engineering, 2016, 152, 14-27.	1.9	54
126	Effects of <i>β</i> â€hydroxybutyricacid on the synthesis and assembly of very lowâ€density lipoprotein in bovine hepatocytes <i>inÂvitro</i> . Journal of Animal Physiology and Animal Nutrition, 2016, 100, 331-336.	1.0	1

#	Article	IF	CITATIONS
127	Prediction of soil attributes using the Chinese soil spectral library and standardized spectra recorded at field conditions. Soil and Tillage Research, 2016, 155, 492-500.	2.6	71
128	Farmland productivity and its application in spatial zoning of agricultural production: a case study in Zhejiang province, China. Environmental Earth Sciences, 2016, 75, 1.	1.3	5
129	A global spectral library to characterize the world's soil. Earth-Science Reviews, 2016, 155, 198-230.	4.0	546
130	Mapping Horizontal and Vertical Spatial Variability of Soil Salinity in Reclaimed Areas. Springer Environmental Science and Engineering, 2016, , 33-45.	0.1	0
131	Baseline estimates of soil organic carbon by proximal sensing: Comparing design-based, model-assisted and model-based inference. Geoderma, 2016, 265, 152-163.	2.3	62
132	Assimilating satellite imagery and visible–near infrared spectroscopy to model and map soil loss by water erosion in Australia. Environmental Modelling and Software, 2016, 77, 156-167.	1.9	106
133	Characterization of field scale soil variability using remotely and proximally sensed data and response surface method. Stochastic Environmental Research and Risk Assessment, 2016, 30, 859-869.	1.9	8
134	Prediction of soil organic matter using a spatially constrained local partial least squares regression and the <scp>C</scp> hinese vis– <scp>NIR</scp> spectral library. European Journal of Soil Science, 2015, 66, 679-687.	1.8	138
135	Improved estimates of organic carbon using proximally sensed vis– <scp>NIR</scp> spectra corrected by piecewise direct standardization. European Journal of Soil Science, 2015, 66, 670-678.	1.8	49
136	Mapping Spatial Variability of Soil Salinity in a Coastal Paddy Field Based on Electromagnetic Sensors. PLoS ONE, 2015, 10, e0127996.	1.1	27
137	Accounting for the effects of water and the environment on proximally sensed vis– <scp>NIR</scp> soil spectra and their calibrations. European Journal of Soil Science, 2015, 66, 555-565.	1.8	133
138	Potential of VIS-NIR-SWIR Spectroscopy from the Chinese Soil Spectral Library for Assessment of Nitrogen Fertilization Rates in the Paddy-Rice Region, China. Remote Sensing, 2015, 7, 7029-7043.	1.8	23
139	In Situ Measurements of Organic Carbon in Soil Profiles Using vis-NIR Spectroscopy on the Qinghai–Tibet Plateau. Environmental Science & Technology, 2015, 49, 4980-4987.	4.6	81
140	Characterizing anisotropic scale-specific variations in soil salinity from a reclaimed marshland in China. Catena, 2015, 131, 64-73.	2.2	19
141	Humoral immunocompetence shifts in response to developmental stage change and mating access in <i>Bactrocera dorsalis</i> Hendel (Diptera: Tephritidae). Bulletin of Entomological Research, 2015, 105, 166-172.	0.5	3
142	Mapping soil salinity in the Yangtze delta: REML and universal kriging (E-BLUP) revisited. Geoderma, 2015, 237-238, 71-77.	2.3	51
143	Estimating spatially downscaled rainfall by regression kriging using TRMM precipitation and elevation in Zhejiang Province, southeast China. International Journal of Remote Sensing, 2014, 35, 7775-7794.	1.3	53
144	Identification of novel kinase inhibitors by targeting a kinaseâ€related apoptotic protein–protein interaction network in HeLa cells. Cell Proliferation, 2014, 47, 219-230.	2.4	13

#	Article	IF	CITATIONS
145	Forbidden-line spectroscopy of the ground-state configuration of Cd-like W. Physical Review A, 2014, 90, .	1.0	32
146	Development of a national VNIR soil-spectral library for soil classification and prediction of organic matter concentrations. Science China Earth Sciences, 2014, 57, 1671-1680.	2.3	143
147	A Layered Perovskite EuBaCo ₂ O _{5+δ} for Intermediateâ€Temperature Solid Oxide Fuel Cell Cathode. Fuel Cells, 2014, 14, 979-990.	1.5	23
148	In Situ Measurement of Some Soil Properties in Paddy Soil Using Visible and Near-Infrared Spectroscopy. PLoS ONE, 2014, 9, e105708.	1.1	62
149	Application of digital soil mapping methods for identifying salinity management classes based on a study on coastal central China. Soil Use and Management, 2013, 29, 445-456.	2.6	36
150	Mapping the three-dimensional variation of soil salinity in a rice-paddy soil. Geoderma, 2013, 195-196, 31-41.	2.3	76
151	<i>In silico</i> analysis of molecular mechanisms of legume lectinâ€induced apoptosis in cancer cells. Cell Proliferation, 2013, 46, 86-96.	2.4	24
152	Integrating Remote Sensing and Proximal Sensors for the Detection of Soil Moisture and Salinity Variability in Coastal Areas. Journal of Integrative Agriculture, 2013, 12, 723-731.	1.7	21
153	Definition of Management Zones for Enhancing Cultivated Land Conservation Using Combined Spatial Data. Environmental Management, 2013, 52, 792-806.	1.2	22
154	Assessment and mapping of soil nitrogen using Visible-Near-Infrared (Vis-NIR) spectra. , 2013, , .		2
155	Genetic structure of silver pomfret (<i>Pampus argenteus</i> (Euphrasen, 1788)) in the Arabian Sea, Bay of Bengal, and South China Sea as indicated by mitochondrial COI gene sequences. Journal of Applied Ichthyology, 2013, 29, 733-737.	0.3	8
156	Experimental and theoretical study of the ground-state <mml:math xmlns:mml="http://www.w3.org/1998/Math/MathML" display="inline"><mml:mi>M</mml:mi>1 transition in Ag-like tungsten. Physical Review A, 2012, 86, .</mml:math 	1.0	34
157	VIS-NIR reflectance spectroscopy of the organic matter in several types of soils. Hongwai Yu Haomibo Xuebao/Journal of Infrared and Millimeter Waves, 2012, 31, 277-282.	0.2	19
158	Methodology Comparison for Effective LAI Retrieving Based on Digital Hemispherical Photograph in Rice Canopy. International Federation for Information Processing, 2011, , 71-82.	0.4	0
159	Comprehensive Evaluation of Tobacco Ecological Suitability of Henan Province Based on GIS. Agricultural Sciences in China, 2010, 9, 583-592.	0.6	36
160	Three Dimensional Variability of Soil Electrical Conductivity Based on Electromagnetic Induction Approach. , 2010, , .		0
161	River bed identification for checkâ€dam engineering using SPOTâ€5 image in the HongShiMao watershed of the Loess Plateau, China. International Journal of Remote Sensing, 2009, 30, 1853-1865.	1.3	13
162	Determination of potential management zones from soil electrical conductivity, yield and crop data. Journal of Zhejiang University: Science B, 2008, 9, 68-76.	1.3	41

#	Article	IF	CITATIONS
163	Potential of Multitemporal ERS-2 SAR Imagery for Land Use Mapping in Coastal Zone of Shangyu City, China. Journal of Coastal Research, 2008, 241, 170-176.	0.1	12
164	Modeling of Cotton Yields in the Amu Darya River Floodplains of Uzbekistan Integrating Multitemporal Remote Sensing and Minimum Field Data. Agronomy Journal, 2007, 99, 1317-1326.	0.9	23
165	ARGIS: An agricultural resource geographic information system for siteâ€specific management of reclaimable saline soils. New Zealand Journal of Agricultural Research, 2007, 50, 813-821.	0.9	3
166	Delineation of Site-Specific Management Zones Based on Temporal and Spatial Variability of Soil Electrical Conductivity. Pedosphere, 2007, 17, 156-164.	2.1	33
167	Quantifying Land Use Change in Zhejiang Coastal Region, China Using Multi-Temporal Landsat TM/ETM+ Images. Pedosphere, 2007, 17, 712-720.	2.1	44
168	Improved Prediction and Reduction of Sampling Density for Soil Salinity by Different Geostatistical Methods. Agricultural Sciences in China, 2007, 6, 832-841.	0.6	34
169	Optimised Spatial Sampling Scheme for Soil Electriclal Conductivity Based on Variance Quad-Tree (VQT) Method. Agricultural Sciences in China, 2007, 6, 1463-1471.	0.6	10
170	Measurement and simulation of biâ€directional reflectance on three zonal soils in the southâ€east of China. New Zealand Journal of Agricultural Research, 2007, 50, 1177-1185.	0.9	5
171	Delineation of site-specific management zones using fuzzy clustering analysis in a coastal saline land. Computers and Electronics in Agriculture, 2007, 56, 174-186.	3.7	163
172	Assessment and mapping of environmental quality in agricultural soils of Zhejiang Province, China. Journal of Environmental Sciences, 2007, 19, 50-54.	3.2	167
173	Evaluating reclamation levels of coastal saline soil using laboratory hyperspectral data. Eurasian Soil Science, 2007, 40, 1095-1101.	0.5	5
174	Application of artificial neural network approach and remotely sensed imagery for regional eco-environmental quality evaluation. Environmental Monitoring and Assessment, 2007, 128, 217-229.	1.3	9
175	Genetic algorithm-based decision tree classifier for remote sensing mapping with SPOT-5 data in the HongShiMao watershed of the loess plateau, China. Neural Computing and Applications, 2007, 16, 513-517.	3.2	11
176	Assessing Reclamation Levels of Coastal Saline Lands with Integrated Stepwise Discriminant Analysis and Laboratory Hyperspectral Data. Pedosphere, 2006, 16, 154-160.	2.1	32
177	Assessment of temporal and spatial variability of soil salinity in a coastal saline field. Environmental Geology, 2005, 48, 171-178.	1.2	51
178	Title is missing!. Precision Agriculture, 2003, 4, 69-86.	3.1	15
179	Detection of Coastal Saline Land Uses with Multi-Temporal Landsat Images in Shangyu City, China. Environmental Management, 2002, 30, 142-150.	1.2	45
180	Temporal changes in the spatial distributions of some soil properties on a temperate grassland site. Soil Use and Management, 2002, 18, 353-362.	2.6	8

#	Article	IF	CITATIONS
181	Temporal changes in the spatial distributions of some soil properties on a temperate grassland site. Soil Use and Management, 2002, 18, 353-362.	2.6	19
182	Title is missing!. Precision Agriculture, 2000, 2, 347-357.	3.1	23
183	Integrating Multi-Temporal Spectral and Structural Information from ALOS/AVNIR-2 Images to Map Heterogeneous Land Use/Cover: A Hybrid Approach. Key Engineering Materials, 0, 500, 640-645.	0.4	0